Patterns of Modulation in the Activity and Connectivity of Motor Cortex during the Repeated Generation of Movement Sequences

Ella Gabitov[1], David Manor[1,2], and Avi Karni[1,2]

Abstract

■ It is not clear how the engagement of motor mnemonic processes is expressed in online brain activity. We scanned participants, using fMRI, during the paced performance of a finger-to-thumb opposition sequence (FOS), intensively trained a day earlier (T-FOS), and a similarly constructed, but novel, untrained FOS (U-FOS). Both movement sequences were performed in pairs of blocks separated by a brief rest interval (30 sec). We have recently shown that in the primary motor cortex (M1) motor memory was not expressed in the average signal intensity but rather in the across-block signal modulations, that is, when comparing the first to the second performance block across the brief rest interval. Here, using an M1 seed, we show that for the T-FOS, the M1–striatum functional connectivity decreased across blocks; however, for the U-FOS, connectivity within the M1 and between M1 and striatum increased. In addition, in M1, the pattern of within-block signal change, but not signal variability per se, reliably differentiated the two sequences. Only for the U-FOS and only within the first blocks in each pair, the signal significantly decreased. No such modulation was found within the second corresponding blocks following the brief rest interval in either FOS. We propose that a network including M1 and striatum underlies online motor working memory. This network may promote a transient integrated representation of a new movement sequence and readily retrieves a previously established movement sequence representation. Averaging over single events or blocks may not capture the dynamics of motor representations that occur over multiple timescales. ■

INTRODUCTION

The primary motor cortex (M1) not only controls specific movements (Georgopoulos, Kalaska, Caminiti, & Massey, 1982) but also coordinates among them to generate meaningful sequences (Ben-Shaul et al., 2004; Tanji, 2001; Carpenter, Georgopoulos, & Pellizzer, 1999; Karni et al., 1998; Nudo, Milliken, Jenkins, & Merzenich, 1996). There is evidence suggesting that lower-level motor areas, including M1, not only generate the pattern of muscle activity necessary to implement action plans but may also play an active role in both the acquisition and retention of complex motor skills in mammalian brains (Peters, Chen, & Komiyama, 2014; Yang et al., 2014; Xu et al., 2009; Yang, Pan, & Gan, 2009; Matsuzaka, Picard, & Strick, 2007; Ben-Shaul et al., 2004; Kleim et al., 2004; Carpenter et al., 1999; Nudo et al., 1996). Animal studies indicate that practice on a motor task may lead to rapid, but long-lasting, synaptic reorganization in M1 (Yang et al., 2009, 2014; Xu et al., 2009). These experience-driven synaptic modifications did not occur with motor activity alone (Yang et al., 2014; Xu et al., 2009) and were correlated with delayed behavioral improvement (Xu et al., 2009; Yang et al., 2009). Human studies using repetitive TMS and anodal transcranial direct current stimulation suggest that increasing the excitability of M1 during practice can improve motor sequence learning (Saucedo Marquez, Zhang, Swinnen, Meesen, & Wenderoth, 2013; Kantak, Mummidisetty, & Stinear, 2012; Stagg, Jayaram, et al., 2011; Vines, Nair, & Schlaug, 2006; Kim, Park, Ko, Jang, & Lee, 2004; Nitsche et al., 2003). These beneficial effects on motor performance were specific to the trained movement sequence (Stagg, Jayaram, et al., 2011; Nitsche et al., 2003) and could not be induced by elevating excitability in premotor and prefrontal cortices (Kantak et al., 2012; Nitsche et al., 2003). Furthermore, fMRI resting state studies have shown an increase in the amplitude of signal fluctuation within the contralateral M1 as well as changes in its functional connectivity following a single session of motor training, suggesting early experience-dependent changes in the representation of the movements within the primary motor cortex (Tung et al., 2013; Vahdat, Darainy, Milner, & Ostry, 2011).

Imaging studies in which multiple training sessions were afforded suggested, in line with animal studies (Matsuzaka et al., 2007; Kleim et al., 2004; Nudo et al., 1996), that a learning-related relative enhancement in the extent of the average M1 signal for a trained versus an untrained movement sequence may become apparent only after multisession training (Steele & Penhune, 2010;

[1]University of Haifa, Haifa, Israel, [2]C. Sheba Medical Center, Ramat Gan, Israel

Floyer-Lea & Matthews, 2005; Penhune & Doyon, 2002; Karni et al., 1995, 1998). However, early phases of practice on motor sequences were reported to be reflected in decreased (Floyer-Lea & Matthews, 2005), increased (Orban et al., 2011; Penhune & Doyon, 2005), or unchanged (Steele & Penhune, 2010; Toni, Krams, Turner, & Passingham, 1998; Karni et al., 1995) magnitude of the mean BOLD-fMRI signal in the M1 contralateral to the performing hand. Decreasing activation putatively reflects reduced recruitment of unspecific neuronal resources, whereas increasing activation is thought to reflect the recruitment and evolution of additional neuronal substrates with practice; the former presumably relate to the setting of more efficient task representation with repeated experience (Poldrack, 2000) whereas the latter relate to the establishment and development of task-specific representations with continued practice (Karni et al., 1998). However, the setting up of more efficient representation of the skill may occur concurrently with increased neural recruitment, making the interpretation of learning-related changes in the averaged activity difficult. An alternative approach was proposed (Gabitov, Manor, & Karni, 2014; Karni et al., 1998) to assess the short-term dynamics, rather than the averaged activity, in a given area or circuit. Short-term dynamic changes in M1 have been shown to be induced by both the excitation of premotor cortical efferents (Davare, Montague, Olivier, Rothwell, & Lemon, 2009; Bestmann et al., 2008; Davare, Lemon, & Olivier, 2008) and by the repetition of experience upon the repeated generation of a movement sequence after a brief interval of rest (Gabitov et al., 2014; Karni et al., 1995). A short-term but reproducible reduction in activity as a function of task repetition (repetition suppression, RS) was shown to occur in M1 in a variety of motor tasks (Chouinard & Goodale, 2009; Hamilton & Grafton, 2009; Dinstein, Hasson, Rubin, & Heeger, 2007; Grafton & Hamilton, 2007; Karni et al., 1995). Thus, the pattern and magnitude of short-term brain activity modulations upon task repetition, RS or repetition enhancement (RE), rather than the averaged evoked signal per se, may constitute a signature for the level of experience with specific movement sequence.

We have recently shown that in M1 the previous experience with a motor sequence was not expressed in the average signal intensity but rather in reproducible signal modulations when comparing activity in performance blocks before and after a brief rest interval (Gabitov et al., 2014). Here, we explored changes in connectivity in performance blocks before and after a brief rest interval, between an M1 seed and other brain regions. We tested whether novelty or experience is reflected in modulations of connectivity across blocks by comparing an untrained to a trained movement sequence. In addition, we tested the hypothesis that short-term signal modulations, within performance blocks as well as across blocks, follow a consistent pattern and may provide a signature for the engagement of motor mnemonic processes during early motor sequence learning in M1. Finally, we tested whether changes in the temporal variability of neural activity reflect the accumulation of experience with the task (He, 2013; Garrett, Kovacevic, McIntosh, & Grady, 2010, 2011; Stein, Gossen, & Jones, 2005). In the scanner, participants performed two movement sequences, a novel, untrained and a previously trained sequence (U-FOS and T-FOS, respectively). Both sequences were composed of the same component movements and were performed at an identical, paced rate, using the left, nondominant hand.

METHODS

The data from the study reported by Gabitov et al. (2014) were used in the current study.

Participants

Thirty-two healthy young adults participated in the current study for payment: 17 participants (19–35 years, 25.7 ± 4.4, mean ± *SD*, five women) in the fMRI group and 15 participants (n = 15, 20–35 years, 25.47 ± 2.73, mean ± *SD*, eight women) in the control group. Both groups were trained and behaviorally tested in an identical protocol, but only participants of the fMRI group underwent an additional imaging session. Thus, the control group was tested to evaluate the possible effects on subsequent performance of the additional experience afforded during the fMRI session. Two participants from the fMRI group were not included in the analysis: One had difficulties with executing the task in the scanner, and another withdrew from the fMRI session for personal reasons. All participants reported no prior history of neurological or psychiatric illness or brain injury and no addiction to drugs, alcohol, or cigarettes (nonsmokers or occasional smokers). Exclusion criteria included current or chronic use of medication, any known learning disabilities and attention-deficit disorder. Only individuals with little (less than 2 years) or no formal music training participated in the current study. Professional typists were excluded as well. All participants affirmed that they had no sleep disorders and reported at least 6 hr of proper night sleep during the study period. Each participant was identified as strongly right-handed using the Edinburg Handedness Inventory (Oldfield, 1971). Before the study, all participants gave written informed consent according to a protocol approved by the C. Sheba Medical Center's Ethics Committee.

Design and Procedures

Participants were trained to accurately perform a given five-element finger-to-thumb opposition sequence (FOS), either sequence A or sequence B, with their nondominant left hand (Figure 1A). Both sequences consisted of identical component movements and were mirror-reversed in relation to each other. Thus, the two sequences were matched for the number of movements per digit and

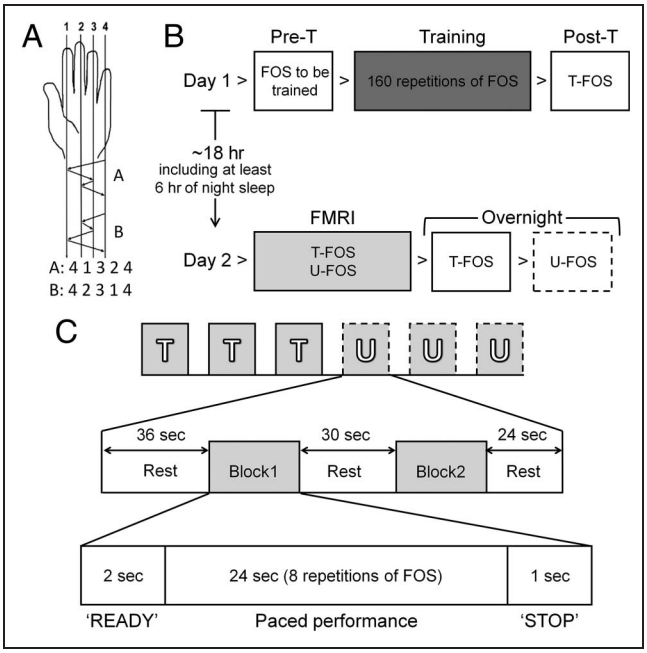

Figure 1. Study design. (A) FOS. The two sequences were matched for a number of movements per digit and mirror-reversed in relation to each other (in terms of order). (B) The overall study design. Day 1: a pretraining performance test (Pre-T), a structured training session (Training: 10 blocks, 16 repetitions of a given sequence per block), and an immediate posttraining performance test (Post-T). Day 2: performance tests of the trained sequence and the untrained sequence (Overnight: T-FOS and U-FOS, respectively). Only participants of the fMRI group took part in the scanning session (fMRI), immediately preceding overnight performance tests. The control (non-fMRI) group was tested to evaluate the effect of the additional experience afforded during the fMRI session on subsequent performances. (C) The fMRI session design. T = T-FOS; U = U-FOS; Block1, Block2 = two blocks of FOS performance. Note that both sequences were performed at an identical auditory-paced rate of 1.66 Hz per movement.

differed only in their order. If the sequence assigned for training was A (T-FOS), then sequence B was used as the novel untrained sequence (U-FOS) and vice versa. The movement sequence was randomly assigned and explicitly instructed. In all sessions and tests, the participants performed the instructed movement sequence lying supine. The executing hand was positioned beside the trunk in direct view (palm-up) of a video camera to allow the recording of all digit movements. Visual feedback was not afforded at any time.

Each participant took part in two study sessions conducted on two consecutive days, separated by 18 hr of interval that included nocturnal sleep (Figure 1B). On Day 1, all participants were trained and tested according to a standard FOS training protocol (Korman et al., 2007; Korman, Raz, Flash, & Karni, 2003). For details, see our previous report (Gabitov et al., 2014). On the second day, all participants were retested on the performance of the trained sequence and then the untrained sequence (Overnight: T-FOS and U-FOS, respectively) using the trained (left) as well as the untrained (right) hand. The results for the untrained hand will be reported elsewhere.

The performance test for each condition included four consecutive blocks of 30 sec of duration separated by 30 sec of rest intervals. Before each test block, participants were asked to perform the movement sequence, and the block was initiated only after the FOS was accurately reproduced three times. Each test block was initiated and terminated by an auditory "READY" and "STOP" signal, respectively. Participants were instructed to perform the sequence continuously "as fast and as accurately as possible." Participants were instructed that in case of an error being noted "not to correct errors but rather to continue from the initial movement of the assigned sequence as smoothly as possible." No feedback on performance was provided. The participants' performance during the test blocks was recorded by a video camera and scored offline. For each test block, two measures of performance were determined from these recordings: (1) the number of correctly completed sequences as a measure of speed and (2) the number of incorrect sequences (errors) as a measure of accuracy.

Before the overnight performance tests, participants of the fMRI group took part in a scanning session, wherein they were asked to perform either the novel sequence (U-FOS) or the sequence trained the day before (T-FOS), using their trained (left) hand. The untrained (right) hand was subsequently tested as well; the results are to be reported elsewhere. The imaging session consisted of three consecutive runs for each sequence (Figure 1C). In this way, potential effects of proactive interference and contextual retrieval that could be caused by switching between the two sequences were minimized (Kiesel et al., 2010; Cothros, Köhler, Dickie, Mirsattari, & Gribble, 2006). The order of sequences was counterbalanced across participants. Experimental runs (each 144 sec long) were separated by a 1.5- to 2-min break, which included a verbal interaction with the participant. The component movements of the sequences were paced by an auditory signal at a fixed rate of 1.66 Hz to control rate-related changes in the BOLD signal (Rao et al., 1996). The paced performance enabled the assessment of signal differences as a function of the order of the component movements minimizing potential differences between the U-FOS and T-FOS that were expected to result from training on one but not on the other sequence (Korman et al., 2003; Karni et al., 1995) as well as minimizing differences in performance rates between individuals. Each imaging run was initiated only after the explicitly designated FOS was accurately reproduced three times. The run consisted of two performance blocks (Block1 and Block2) separated by a rest interval of 30 sec. Each block was initiated by an auditory and visual "READY" cue (2 sec), after which participants performed the required FOS continuously in a paced manner for a total of eight repetitions of the FOS (24 sec). The end of the performance block was marked by an auditory and visual "STOP" cue (1 sec).

The participants' performance during the fMRI session was recorded by a video camera focused on the

performing hand and evaluated by at least one trained observer, online and offline. Performance was evaluated for accuracy, timing (i.e., initiation and termination of FOS performance) and performance rate to ensure an appropriate task execution. Errors occurred very rarely and when noted by the experimenters or the participants, the run was repeated. No additional errors were observed during evaluation of performance offline. Only runs with errorless performance were included in the analyses. This experiment was realized using Cogent 2000 developed by the Cogent 2000 team at the FIL and the ICN and Cogent Graphics developed by John Romaya at the LON, Wellcome Department of Imaging Neuroscience and implemented in MATLAB (The Mathworks, Inc., Natick, MA).

fMRI Data Acquisition and Analyses

Acquisition Parameters

fMRI scanning was carried out at the C. Sheba Medical Center, Tel-Hashomer, using a 3-T whole-body high-definition system (GE Excite 3 HD, Fairfield, CT) equipped with an eight-channel head coil. A high-resolution full-brain 3-D structural images were acquired in the axial orientation using a T1*-weighted echo-planar sequence (repetition time = 7.3 msec, echo time = 3 msec, flip angle = 20°, field of view = 256 × 256 mm^2, matrix size = 256 × 256 voxels, voxel size = 1 × 1 × 1 mm^3). BOLD-sensitive functional images were obtained using a gradient-echo planar T2*-sequence (repetition time = 3000 msec, echo time = 35 msec, flip angle = 90°, field of view = 220 × 220 mm^2, matrix size = 64 × 64 voxels, voxel size = 3.4 × 3.4 × 3.4 mm^3, no gap, ascending) with 40 axial oblique slices, covering the whole brain.

Preprocessing

The structural and functional images were converted to Neuroimaging Informatics Technology Initiative (NIfTI) format using MRIcron (University of South Carolina). Preprocessing and statistical analysis of the data were carried out with Statistical Parametric Mapping (SPM8; Wellcome Department of Cognitive Neurology, London, UK) operating under Matlab R2012a. For each run, the four initial scans were discarded to allow for magnetic saturation and equilibration effects. All images were reorientated to stereotactic space. Functional data were realigned and unwarped, adjusting for interactions between movement and local field inhomogeneity (Hutton, Andersson, Deichmann, & Weiskopf, 2013; Andersson, Hutton, Ashburner, Turner, & Friston, 2001). Normalization to the Montreal Neurological Institute (MNI) space was performed using parameters obtained from the segmentation procedure of the structural data, following co-registration. The normalized functional images were resampled to voxel dimensions of 3 mm^3. Finally, functional images were spatially smoothed with a Gaussian kernel of 8 mm FWHM. Before statistical analyses, head motion artifact detection was applied to the preprocessed data using the Artifact Detection Tools (Mazaika, Hoeft, Glover, & Reiss, 2009). No significant head motion artifacts were detected (normalized z-threshold = 2, movement threshold = 2 mm, rotation threshold = 0.05 rad).

Whole-brain Analyses

Statistical analyses of BOLD signal changes were performed using a general linear model (GLM; Friston et al., 1995). Individual models were specified separately for each sequence (U-FOS, T-FOS) using a multisession design while each session included data from a single run (three runs). Regressors of interest for each performance block (Block1, Block2) were modeled as a boxcar function with a length of 24 sec convolved with the canonical hemodynamic response function. A high pass filter of 128 sec was used to remove low-frequency noise. For the block design, inclusion of motion covariates has a deleterious impact on GLM sensitivity when even moderate correlation existed between motion and the experimental design (Johnstone et al., 2006). Therefore, movement parameters derived from realignment of the functional volumes were not included as covariates. Following the model parameters estimation, a linear contrast for performance-related changes in BOLD-fMRI signal was defined for each sequence versus rest (U-FOS > Rest, T-FOS > Rest). The individual contrast images were introduced to a second-level random effects analysis, separately for each sequence, using a one-sample t test.

ROI Definition

Because of intersubject anatomical variability (Nieto-Castañón & Fedorenko, 2012; Fedorenko, Hsieh, Nieto-Castañón, Whitfield-Gabrieli, & Kanwisher, 2010; Woods, 1996) and the variability in the representation of hand movements within the motor cortex of a given individual (Nudo et al., 1996; Schlaug, Knorr, & Seitz, 1994; Nudo, Jenkins, Prejean, & Grenda, 1992), the ROI within M1 was defined in each individual brain using a combined anatomical and functional approach. The central sulcus and the hand knob (Yousry et al., 1997), contralateral to the performing hand, were used for anatomical identification of the primary motor hand area of each individual. The functional voxels relevant to the task performance were identified on an individual level from activation maps of a whole-brain analysis for each sequence (U-FOS > Rest, T-FOS > Rest) using family-wise error rate (FWE) correction at $p < .05$. The MNI coordinates of the most active voxel (local maxima) within the right M1 hand area, corresponding to the performing hand, were then extracted for each individual and each sequence. Individual ROIs were defined as a sphere centered at mean

MNI coordinates across the two sequences with a radius of 6 mm.

Functional Connectivity Analyses

A seed-driven approach was applied to explore changes in functional connectivity during FOS performance. Individual ROIs within M1 were used as a seed. Connectivity analyses on preprocessed functional images were run using the Functional Connectivity Toolbox (Conn) for SPM (Whitfield-Gabrieli & Nieto-Castanon, 2012). This toolbox allows condition-dependent functional connectivity analysis (e.g., for resting state network analyses and block design studies). Before connectivity analyses, the data underwent additional temporal preprocessing. Six parameters obtained by rigid body head motion correction (three rotation and three translation parameters) plus six additional parameters representing the corresponding first-derivative terms were used as temporal covariates to reduce the impact of motion within performance blocks. Main effect of block may affect within-block connectivity estimates in the presence of possible voxel-specific differences in hemodynamic delay. Therefore, main effect of each block (Block1, Block2; each block 24 sec long convolved with the canonical hemodynamic response function) and the corresponding first-derivative terms were included as additional temporal confounding factors. Temporal covariates were removed from the BOLD functional data using linear regression. The resulting residual BOLD time series were band-pass filtered (0.008 Hz $< f <$ 0.1 Hz).

The preprocessed BOLD time series were divided into scans associated with each block (Block1, Block2) separately for each sequence (U-FOS, T-FOS). To take into account the hemodynamic delay, block regressors were convolved with a canonical hemodynamic response function and rectified. Temporal connectivity maps were generated for each block (Block1, Block2) separately for each sequence (U-FOS, T-FOS) by estimating Pearson's correlation coefficients between the BOLD signal from the seed region (i.e., ROI within the M1) and that at every other brain voxel. All seed-to-voxel correlation coefficients were converted to normally distributed scores using Fisher's transformation to allow for second level GLM analyses. The whole-brain connectivity patterns with the M1 seed were tested in second-level analyses for the main effect of sequence (U-FOS > T-FOS, U-FOS < T-FOS), the main effect of block (Block1 > Block2, Block1 < Block2), and directional sequence by block interactions, that is, testing for a greater increase in connectivity (with the M1 seed) across blocks, during the U-FOS performance compared with the T-FOS performance ([U-FOS: Block1 < Block2] × [T-FOS: Block1 > Block2]) and vice versa ([U-FOS: Block1 > Block2] × [T-FOS: Block1 < Block2]).

Connectivity maps generated from the second level GLM analyses were thresholded at $p \leq .001$ and overlaid on the mean structural image of all participants or the surface rendered from the participants' mean structural segmented images using SPM8 and Functional Imaging Visualization Environment (FIVE; nmr.mgh.harvard.edu/harvardagingbrain/People/AaronSchultz/OrthoView.html). Statistical inferences were performed on the peak-level using p values FWE-corrected for multiple comparisons over a small VOI. Areas of interest for small volume corrections were defined, for structures within the motor-related (Hardwick, Rottschy, Miall, & Eickhoff, 2013; Halsband & Lange, 2006) network, as follows: (1) the right sensorimotor cortex, defined as a union between the right primary sensory and motor cortices using human motor area template (Mayka, Corcos, Leurgans, & Vaillancourt, 2006) as well as (2) the right and (3) the left putamen using automated anatomical labeling (AAL; Tzourio-Mazoyer et al., 2002). Clusters that survived $p < .05$ (uncorrected) on the cluster level were reported as well. Finally, Fisher-transformed correlation coefficients were calculated for clusters, wherein connectivity with the M1 seed showed significant sequence by block interaction. These correlation coefficients were entered to Statistical Package for the Social Sciences (SPSS Statistics for Windows, Version 19.0; IBM Corp., Armonk, NY) for post hoc analyses applying paired samples t tests. Statistical inferences were performed at 0.05 level corrected for multiple tests (i.e., the number of clusters) using Bonferroni adjustments.

Time-course Analyses

Raw ROI time courses were extracted from preprocessed functional images for each run using the MarsBar toolbox for SPM (Brett, Anton, Valabregue, & Poline, 2002). These raw BOLD signals were converted to percent signal change. To reduce the low-frequency noise because of the scanner drift, the BOLD signal at the performance block's onset ("READY" cue) was used as the block's baseline. To explore within-block dynamics each block was divided into two equal phases (Phase1, Phase2), each consisting of four successive time points (signal measurements), with Phase1 beginning 6 sec after the "READY" cue and Phase2 including the "STOP" cue; exclusion of time points corresponding to the first 6 sec following the "READY" cue minimized the effects of hemodynamic delay.

Analyses of temporal BOLD signal variability were performed on BOLD signals converted to percent signal change relative to the mean evoked signal across all time points for each run. To assess the magnitude of temporal BOLD signal variability, we used the mean squared successive difference (SSD) measure (Von Neumann, Kent, Bellinson, & Hart, 1941). Mean SSD was suggested as a more reliable estimator of the true underlying temporal variability of the BOLD signal, compared with *SD*, with no need for particular assumption about a functional form of the expected signal drift or variation of the mean signal across conditions (Mohr & Nagel, 2010). Individual mean

SSD of percent signal change were calculated separately for each phase within each block (i.e., Phase1 and Phase2 separately for Block1 and Block2) as well as for each rest interval (before Block1, ending in the first "READY" cue; between Block1 and Block2, starting 9 sec after the first "STOP" cue and ending in the second "READY" cue; and after Block2, starting 9 sec after the second "STOP" cue and including the last scan; exclusion of time-points corresponding to the first 9 sec following the "STOP" cue allowed for the hemodynamic response to return to baseline). In addition, BOLD signal variability was analyzed in terms of *SD* for each period of interest (Garrett et al., 2010, 2011). The analyses were designed as within-subject comparisons. Repeated-measures ANOVAs or paired samples *t* tests were run using SPSS. The results were corrected for nonsphericity violation using the Greenhouse–Geisser adjustment.

Behavioral Data Analyses

For each test block two performance measures for each individual were determined: the number of correctly completed sequences as a measure of speed and the number of sequences with ordering errors as a measure of accuracy. For statistical analyses, these measures were averaged across the four test blocks for each performance test. In addition, the slope for speed as a measure of within-test improvement and the *SD* for speed as a measure of within-test variability were determined. The slope was calculated as a gradient of linear regression line through 4 data points; each point represented speed achieved during one test block. The *SD* for speed within each performance test was converted to percentages relative to individual mean speed achieved in that specific test. Unless otherwise stated, the analyses were designed as within-subject comparisons. Separate repeated-measures ANOVAs for each performance measure with sequence (U-FOS, T-FOS) as within-subject factor were run using SPSS. The results were corrected for nonsphericity violation using the Greenhouse–Geisser adjustment.

RESULTS

fMRI Results

The whole-brain analyses did not show significant differences in the performance-driven changes in neural activity between the two sequences (Gabitov et al., 2014). Group effects of performance-related increases in neural activity for each sequence (U-FOS > Rest, T-FOS > Rest) are shown in Figure 2A.

ROI Definition

The MNI coordinates of the most active voxel within the right hemisphere hand knob (Yousry et al., 1997), that is, the primary motor hand area contralateral to the performing hand, did not differ between the two sequences. A repeated-measures multivariate ANOVA with Sequence (U-FOS, T-FOS) as a within-subject factor with three levels, that is, coordinates (*x*, *y*, and *z*), showed no significant effect of Sequence ($F(3, 12) = 1.06$, $p = .40$). Therefore, individual MNI coordinates were averaged across the two sequences for each participant, and the ROI was defined as a sphere ($r = 6$ mm) centered on that mean location (40 ± 0.41, -19 ± 0.82, 54 ± 0.95, mean ± *SEM* for *x*, *y*, and *z*, respectively; Figure 2B).

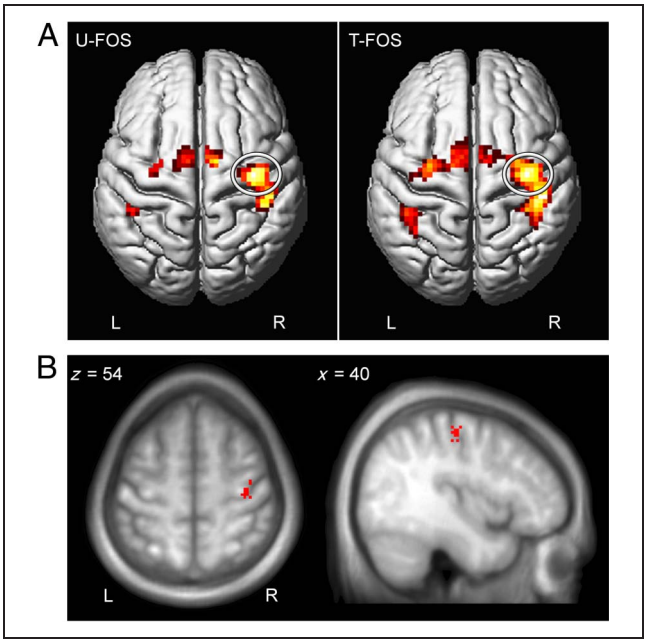

Figure 2. Task-related activity and ROI. (A) Activation maps of group effects showing areas activated during performance of the U-FOS (left) and the T-FOS (right) overlaid on the surface rendered from the mean structural segmented images of all participants. The maps were thresholded using FWE correction at $p < .05$. Ellipse = motor hand area corresponding to the performing hand. (B) Individual locations of the most active voxels averaged across sequences within the M1 hand area were used as a center for sphered ROI with a radius of 6 mm.

Connectivity Analyses

Areas wherein functional connectivity with the M1 seed showed significant effects are listed in Table 1. Comparison of the connectivity maps with the M1 hand area as the seed, generated for the performance blocks during execution of the U-FOS and the T-FOS, showed no significant main effect of Sequence (U-FOS vs. T-FOS). Analyses of the main effect of Block revealed a significant decrease (i.e., Block1 > Block2) in connectivity between the M1 seed and the lateral anterior part of the left inferior frontal gyrus (Table 1, labeled as Frontal_Inf_Orb (AAL)), a cluster conjoining Brodmann's areas (BA) 45, 46, and 47.

The whole-brain connectivity patterns, with the M1 seed, were differentially modulated by the repeated performance of the two sequences (Figure 3 and Table 1).

Table 1. Functional Connectivity with the M1 Seed

		MNI Coordinates					
Label		*x*	*y*	*z*	*Cluster Size (Voxels)*	*z-Score*	*p*
U-FOS > T-FOS							
No significant results		–	–	–	–	–	–
U-FOS < T-FOS							
No significant results		–	–	–	–	–	–
Block1 < Block2							
No significant results		–	–	–	–	–	–
Block1 > Block2							
Frontal_Inf_Orb	L	−48	44	−8	36	3.64	.03
[U-FOS: Block1 < Block2] × [T-FOS: Block1 > Block2]							
Precentral	R	45	−7	43	38	4.31	.02[*1]
Putamen	R	36	−7	−2	52	4.15	<.01[*2]
Putamen	L	−33	−16	−2	74	4.52	$.02_{FWE}$[*3]
Rolandic_Oper	R	60	8	10	54	4.05	<.01
Frontal_Inf_Tri	L	−39	26	7	31	3.93	.03
[U-FOS: Block1 > Block2] × [T-FOS: Block1 < Block2]							
No significant results		–	–	–	–	–	–

Labeling clusters obtained from connectivity maps thresholded at $p < .001$ using AAL (Tzourio-Mazoyer et al., 2002). p_{FWE} = cluster-level FWE-corrected over the entire brain volume; p = cluster-level uncorrected; [*1–*3] = significant peak at .05 level FWE-corrected over a small VOI, [1–3] refers to an area of interest used for small volume correction: [1] the right sensorimotor cortex defined as a union between the right primary sensory and motor cortexes using Human Motor Area Template (Mayka et al., 2006), [2] the right and [3] the left putamen using AAL.

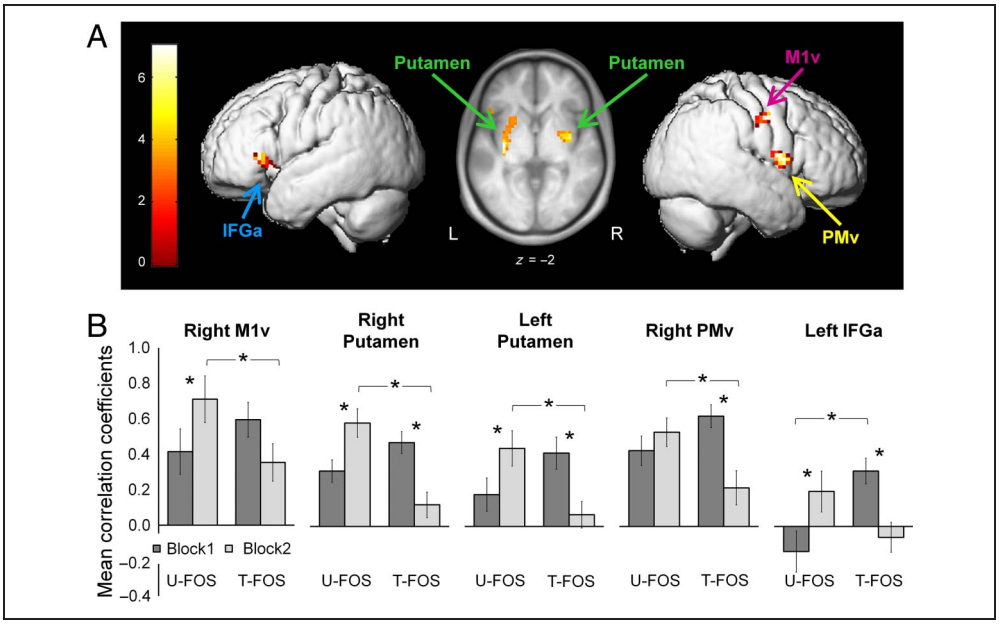

Figure 3. Functional connectivity analyses using M1 hand area as a seed. (A) Areas wherein functional connectivity patterns were differentially modulated by the repeated performance of the two sequences using M1 as a seed (interaction: [U-FOS: Block1 < Block2] × [T-FOS: Block1 > Block2]). Connectivity map of group effects overlaid on the mean structural image of all participants or the surface rendered from the participants' mean structural segmented images. The map was thresholded at $p < .001$. The color bar represents t values. M1v = primary motor cortex ventral to the hand area; PMv = ventral premotor cortex; IFGa = anterior part of the inferior frontal gyrus. (B) Mean correlation coefficients between the M1 seed and each of the clusters, wherein connectivity with the M1 seed showed significant sequence by block interaction. Columns = mean Fisher-transformed correlation coefficients; bars = *SEM*s. *Significant differences at 0.05 level corrected for multiple tests (i.e., a number of clusters) using Bonferroni adjustments.

Overall, there was a pattern of increased connectivity with the M1 seed, across blocks (i.e., comparing the functional connectivity in performance blocks before and after the brief rest intervals), for the U-FOS but a reduction in connectivity for the T-FOS. Analyses of sequence by block interactions showed significant changes only in one direction, toward greater increase in connectivity with the M1 seed across blocks during the U-FOS performance compared with the T-FOS performance ([U-FOS: Block1 < Block2] × [T-FOS: Block1 > Block2]). This interaction was significant for clusters within the right M1 ventral to the hand area and the striatum, bilaterally (Figure 3A and Table 1, labeled as precentral and putamen (AAL), respectively). The peak voxels within the striatum were located in the ventral posterior parts of the putamen, bilaterally, corresponding to the sensorimotor territories of the BG (Lehéricy et al., 2004, 2005). Post hoc analyses showed that across blocks during the U-FOS performance the connectivity between the M1 seed and the right M1 ventral to the hand area increased ($t(14) = 4.11$, $p < .01$; Figure 3B). There was also an increase in the M1 connectivity with the striatum ($t(14) = 3.18$, $p < .05$; $t(14) = 2.92$, $p = .05$, correlation coefficients for the M1 seed with the right and the left putamen, respectively). However, performance of the T-FOS led to a relative decrease in the M1 connectivity with the striatum across blocks ($t(14) = -5.95$, $p < .001$; $t(14) = -3.51$, $p < .05$, correlation coefficients for the M1 seed with the right and the left putamen, respectively; Figure 3B). Additional clusters that showed a significantly greater increase in connectivity with the M1 seed, across blocks, for the U-FOS compared with the T-FOS were located within the right rolandic operculum, corresponding to the ventral premotor cortex (PMv), and the anterior part of the left inferior frontal gyrus (IFGa, BA 45 and 47; Figure 3A and Table 1, labeled as Rolandic_Oper and Frontal_Inf_Tri (AAL), respectively). Post hoc analyses showed a relative increase in the right-M1–left-IFGa connectivity across blocks, during the U-FOS performance ($t(14) = 3.41$, $p < .05$), but a relative decrease in the right-M1–right-PMv as well as the right-M1–left-IFGa connectivity during the performance of the T-FOS ($t(14) = -4.82$, $p < .01$; $t(14) = -4.70$, $p < .01$, correlation coefficients for the M1 seed with the right PMv and the left IFGa, respectively; Figure 3B).

Correlation coefficients with the M1 seed were also compared between the two sequences (U-FOS, T-FOS) separately, for each block (Block1, Block2). Connectivity for the M1 seed with the right M1 area ventral to the hand knob and the striatum was similar for both sequences during the first blocks, but after the brief rest interval during the second blocks in the pairs connectivity was stronger for the U-FOS compared with the T-FOS ($t(14) = 4.18$, $p < .01$; $t(14) = 5.02$, $p < .001$; $t(14) = 3.90$, $p = .01$, correlation coefficients for the M1 seed with the ventral part of the right M1, the right and the left putamen, respectively; Figure 3B). A similar pattern was observed for the right-M1–right-PMv connectivity values ($t(14) = 3.16$, $p < .05$). The right IFGa was the only cluster that showed stronger connectivity with the M1 seed for the T-FOS compared with the U-FOS during the first block ($t(14) = -3.47$, $p < .05$; Figure 3B).

Time-course Analyses

The time-course series, for the two sequences, in terms of percent signal change extracted from the M1 hand area, are shown in Figure 4. A repeated-measures ANOVA with Sequence (U-FOS, T-FOS), Run (1–3), Block (Block1, Block2), and Phase (Phase1, Phase2) as within-subject factors showed no significant effect of Run ($F(1.86, 26.09) = 0.43$, $p = .64$). There were neither significant differences in the magnitude of evoked BOLD signals between the two sequences ($F(1, 14) = 2.75$, $p = .12$) nor a differential modulation of the mean signal across blocks ($F(1, 14) = 0.94$, $p = .35$; $F(1, 14) = 0.53$, $p = .48$, Block effect and Sequence × Block interaction, respectively). Thus, the mean magnitude of the evoked BOLD signal within each block did not differentiate between the two sequences. However, there was a significant Sequence × Block × Phase interaction ($F(1, 14) = 8.62$, $p = .01$) indicating that activity varied between Phase1 and Phase2 as a function of the sequence and its repetition across the brief rest interval.

Post hoc repeated-measures ANOVAs were performed separately for each sequence (U-FOS, T-FOS). Repetition effects across blocks (Block2–Block1) averaged across runs are shown in Figure 4 (bottom middle). On average there was a trend toward relative enhancement (RE) in the BOLD signals across blocks when participants executed the T-FOS; these differences, however, were not significant ($F(1, 14) = 1.28$, $p = .28$). There was a significant Phase × Block interaction only for the U-FOS ($F(1, 14) = 11.18$, $p < .01$; $F(1, 14) = 0.13$, $p = .73$, U-FOS and T-FOS, respectively). Repeated-measures ANOVAs performed separately for each phase (Phase1, Phase2) during the U-FOS performance did not show any significant differences across blocks ($F(1, 14) = 0.22$, $p = .65$; $F(1, 14) = 1.11$, $p = .31$, Phase1 and Phase2, respectively). However, when the phases where compared within blocks, there was a significant reduction of BOLD signal from Phase1 to Phase2 in the first block, that is, within-block RS, ($F(1, 14) = 8.67$, $p = .01$), but no BOLD signal modulation between the two phases in the second, repeated block ($F(1, 14) = 0.25$, $p = .63$; Figure 4A, right plot). No significant changes in the evoked BOLD signals were observed within blocks during the T-FOS performance (Figure 4B, right plot). The differential within-block modulations in the BOLD signal were replicable across runs (Figure 5).

Signal variability within the M1 significantly decreased during the performance of the both sequences compared with rest (Figure 6 and Table 2). A repeated-measures ANOVA on the mean SSD (see Methods) with Sequence (U-FOS, T-FOS), Run (1–3), and Period of interest (Phase1 and Phase2 within each block as well as three periods of

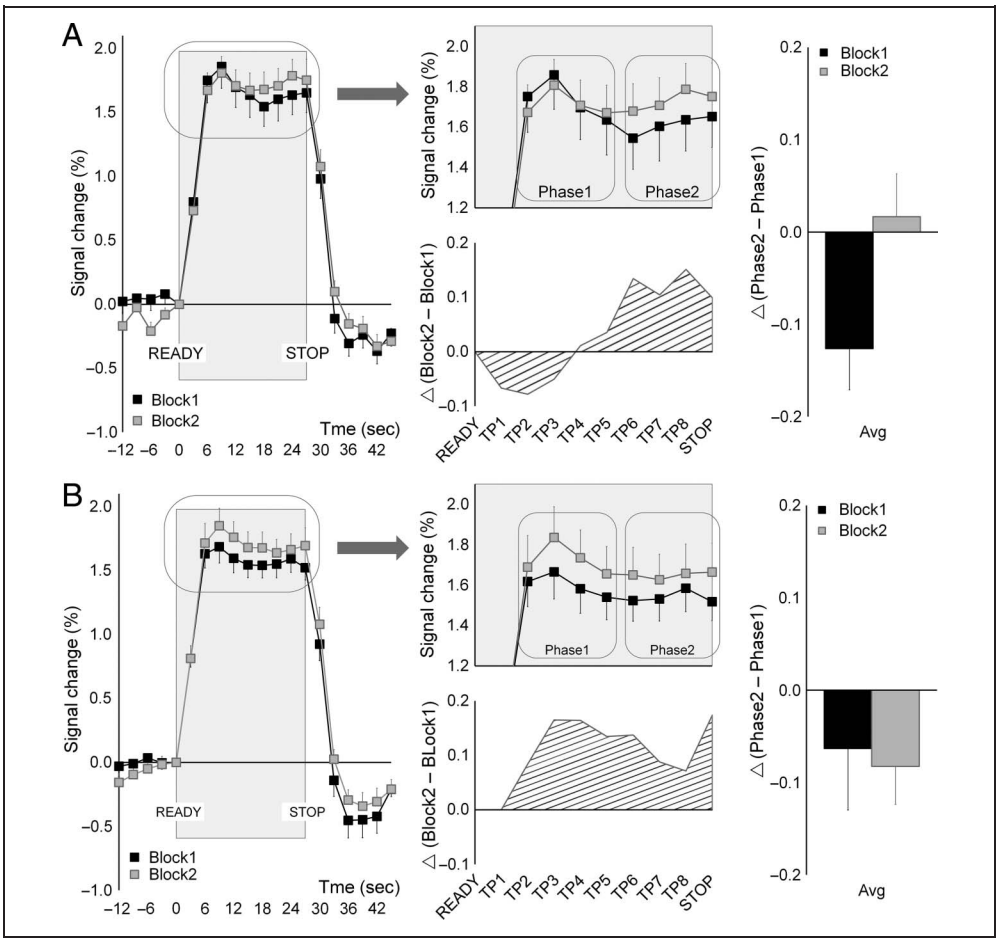

Figure 4. Time courses of BOLD signal within the M1 hand area and repetition effects: (A) U-FOS and (B) T-FOS. Mean time courses in percent signal change (vs. performance onset, "READY" cue) across all sequence-specific runs are plotted separately for each performance block (Block1, Block2) versus time (in seconds, counted from a performance onset, that is, "READY" cue = 0 sec; left and top middle plots). Data points = group mean percent signal changes at a single time-point; bars = *SEM*s. Repetition effects across blocks were measured as differences (△) between the two blocks (i.e., Block2 − Block1; bottom middle plots). Vertices = △ at corresponding time points averaged across runs. Negative values correspond to RS effects across blocks; positive values correspond to RE effects across blocks. Repetition effects within blocks were measured as differences (△) between the two phases (i.e., Phase2 − Phase1; right plots). Columns = within-block repetition effects averaged across runs; bars = *SEM*s.

rest) as within-subject factors resulted in significant effect of Period of interest ($F(1.91, 26.76) = 6.78, p < .01$) irrespective of the sequence ($F(1, 14) = 0.10, p = .76$; $F(2.41, 33.80) = 0.42$, $p = .70$, main effect of Sequence and Sequence × Period-of-interest interaction, respectively) or run ($F(1.82, 25.46) = 0.66, p = .51$). Post hoc pairwise comparisons revealed that variability during all rest periods was significantly higher than during the actual performance blocks (Table 2A). A repeated-measures ANOVA with Sequence (U-FOS, T-FOS), Run (1–3), Block (Block1, Block2), and Phase (Phase1, Phase2) as within-subject factors showed a significant decrease in variability from Phase1 to Phase2 ($F(1, 14) = 22.33, p < .001$) irrespective of a sequence, run, or block.

Analyses of *SD* for each period of interest showed similar results (Figure 6B and Table 2B). Thus, while signal variability within M1 significantly decreased during the performance of the two sequences compared with rest, as well as within blocks (i.e., across phases), the signal variability, within blocks or across blocks, did not reflect sequence specificity.

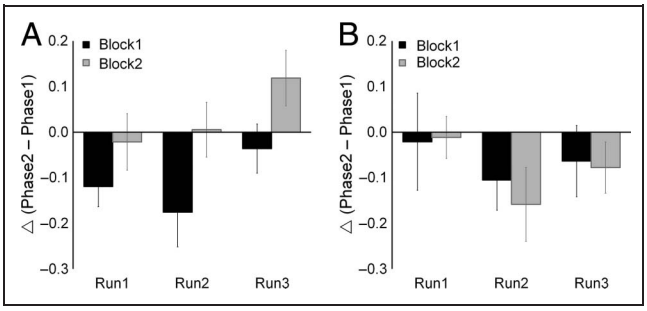

Figure 5. Within-block repetition effects within the M1 hand area for each run: (A) U-FOS and (B) T-FOS. Repetition effects within blocks, measured as differences (△) between the two phases (i.e., Phase2 − Phase1), are plotted separately for each block and run. Columns = within-block repetition effects; bars = *SEM*s.

Behavioral Results

The results of the behavioral performance tests undertaken after the imaging session, in comparison with the nonscanned control group are shown in Figure 7. The performance of the T-FOS was significantly faster, more accurate, and less variable compared with the U-FOS in both groups. A repeated-measures ANOVA with Group (fMRI, control) as a between-subject factor and Sequence (Overnight T-FOS and U-FOS) as a within-subject factor showed a significant effect of Sequence for both, the number of correct sequences (i.e., speed) and the

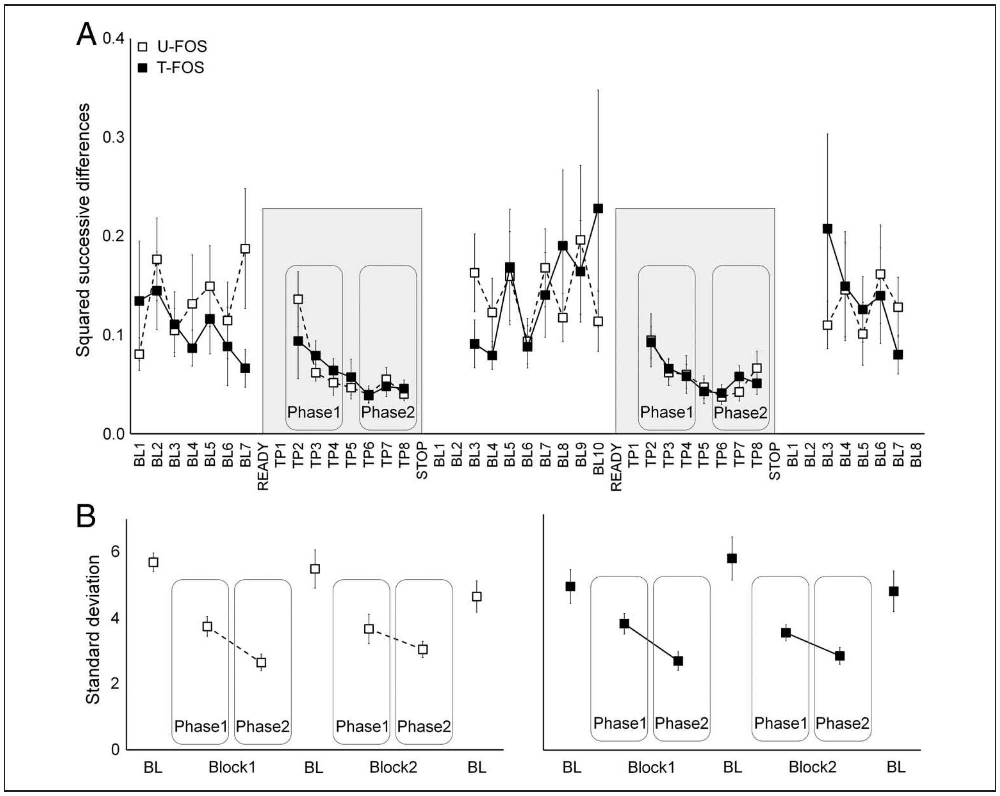

Figure 6. Temporal variability of BOLD signal within the M1 hand area. (A) SSDs averaged across runs are plotted separately for each sequence (U-FOS = white squares; T-FOS = black squares) versus time points with distinct indexing for each period of interest: BL = rest; TP = performance block. Data points = group mean SSD of signal change (%) between the current and the next time-point; bars = *SEM*s. (B) *SD* for each period of interest averaged across runs is plotted separately for each sequence (U-FOS = left plot, T-FOS = right plot). BL = rest; data points = group mean *SD*; bars = *SEM*s.

number of errors ($F(1, 28) = 93.10, p < .001; F(1, 28) = 36.98, p < .001$, respectively). The effect of Sequence was also significant for the within-test rate of improvement in speed (slope) and the within-test speed variability, that is, *SD* ($F(1, 28) = 9.09, p < .01; F(1, 28) = 18.14, p < .001$, respectively). There was no significant Group effect for any of the behavioral measures. However, the analyses of errors and slope showed a significant Sequence × Group interaction ($F(1, 28) = 36.98, p < .001; F(1, 28) = 5.01, p < .05$, respectively). A post hoc *t* test performed separately for each sequence showed significant differences in performance between the two groups only

Table 2. Statistics of Temporal Variability for BOLD Signal within the M1 Hand Area

A. Mean SSDs

Phase	*Rest1 (0.121 ± 0.015)*	*Rest2 (0.143 ± 0.030)*	*Rest3 (0.135 ± 0.032)*	*Phases Difference*
Block1 Phase1 (0.081 ± 0.010)	0.001	0.005	0.015	0.001
Block1 Phase2 (0.045 ± 0.005)	0.001	0.005	0.006	
Block2 Phase1 (0.072 ± 0.008)	0.003	0.008	0.013	0.019
Block2 Phase2 (0.050 ± 0.006)	<0.001	<0.001	0.000	

B. SD

Phase	*Rest1 (5.274 ± 0.340)*	*Rest2 (5.588 ± 0.571)*	*Rest3 (4.683 ± 0.474)*	*Phases Difference*
Block1 Phase1 (3.749 ± 0.231)	<0.001	0.002	0.060	<0.001
Block1 Phase2 (2.648 ± 0.236)	<0.001	<0.001	0.001	
Block2 Phase1 (3.576 ± 0.306)	0.001	0.004	0.056	0.041
Block2 Phase2 (2.923 ± 0.206)	<0.001	<0.001	0.002	

Statistics (*p* values) for mean differences in variability measures (mean SSD and *SD*) between periods of interest (Phase1 and Phase2 for each block as well as three periods of rest) resulted from post hoc pairwise comparisons. Mean values of variability for each period of interest are shown in parentheses (mean ± *SEM*).

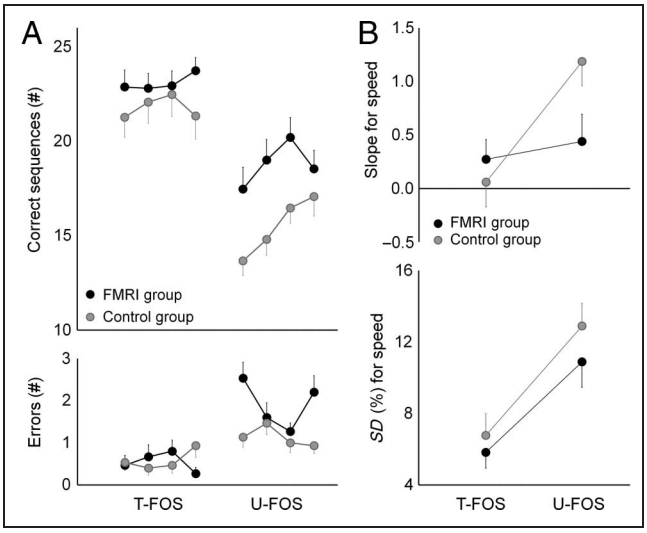

Figure 7. Behavioral results. Performances of fMRI and control group overnight. (A) The number of correctly completed sequences (i.e., speed, top) and the number of sequences with ordering errors (bottom). Data points = group mean values for each of the four test blocks; bars = *SEM*s. (B) Within-test change in speed (slope, top) and within-test speed variability (*SD*, bottom). Data points = group mean values; bars = *SEM*s.

for the U-FOS (Overnight U-FOS). As can be seen in Figure 7, U-FOS performance was faster in the fMRI group with a reduced within-test rate of improvement ($T(28) = 2.61, p = .01$; $T(28) = -2.20, p < .05$, speed and slope, respectively, fMRI vs. control group) indicating that the experience with the novel sequence inside the scanner contributed to the subsequent performance. However, this experience was insufficient to reduce the within-test variability for speed (*SD*) during the subsequent U-FOS performance ($T(28) = -1.05, p = .30$, fMRI vs. control group). The number of errors was significantly higher in the fMRI group ($T(28) = 2.64, p = .01$, fMRI vs. control group), although the size of this effect was very small because of the overall small number of errors committed (1.9 ± 0.23; 1.13 ± 0.18, mean $\pm$ *SEM*, fMRI and control group, respectively). This small difference in accuracy reflected in part the unintended switching to the T-FOS.

DISCUSSION

Our results suggest that short-term BOLD signal modulations, within the performance blocks as well as across blocks separated by the brief rest interval, reflect the level of experience with the movement sequence and may, thus, reliably reflect underlying mnemonic processes. Both the patterns of neural activity and the functional connectivity of the primary motor hand area (contralateral to the performing hand) were differentially modulated by the repeated performance of the untrained and trained sequences. However, different levels of motor experience were not reflected in the averaged signal intensities or in signal variability per se. The transient but consistent patterns of dynamic changes in motor cortex activity and connectivity during the repeated performance of the sequences can be considered as neural signatures of novelty and experience with a motor task.

There were no significant differences between the two sequences in the location of the most active voxel within the primary motor hand area contralateral to the performing hand or in the mean magnitude of activity evoked during the performance. The current results, therefore, are in line with the results of animal studies showing that the representation of motor sequences in M1 may not be reliably assessed by averaging neuronal activity (Zelenin et al., 2011; Ben-Shaul et al., 2004; Hatsopoulos, Paninski, & Donoghue, 2003). There are data suggesting that different tasks can be reliably expressed in the modulation patterns rather than in the population mean of activity of motor cortex neurons (Zelenin et al., 2011), presumably reflecting the fact that the same neuronal pool in the motor cortex can be recruited in different tasks (Yang et al., 2014; Zelenin et al., 2011).

During the performance blocks signal variability in the contralateral M1 significantly decreased, compared with rest as well as within blocks (i.e., across phases), for both sequences (Figure 6). These results are in agreement with recent reports (He, 2013) of a reduction in variability in the fMRI BOLD signals following stimulus onset, as well as with animal studies that showed that intrinsically generated spontaneous fluctuations in neuronal activity undergo suppression during task-evoked activity throughout the cortex in a broad range of conditions (White, Abbott, & Fiser, 2012; Churchland et al., 2010; Churchland, Yu, Ryu, Santhanam, & Shenoy, 2006). The decline in variability implies that cortical circuits can be stabilized by an input or a task and may support information encoding (He, 2013; White et al., 2012; Churchland et al., 2010). In the current study, however, the large decreases in the M1 signal variability with task performance were not differentially modulated by the level of experience with the specific movement sequence or by its repetition across the brief rest interval.

Relative changes in the magnitude of the mean M1 activity across blocks were observed for the T-FOS, with a trend toward RE (Figure 4B). These RE effects have been shown to be significant for participants that expressed delayed "offline" performance gains overnight (i.e., in addition to the gains achieved immediately after the training; Gabitov et al., 2014). RE effects in the M1 contralateral to the performing hand were reported to occur for practiced sequences (Karni et al., 1995, 1998). However, unlike the previous results of Karni et al. (1995, 1998), no across-blocks reductions in the magnitude of the mean M1 activity upon repetition (RS) were observed for the U-FOS in the current study. It has been proposed that RS effects in the primary motor cortex may reflect an adaptation phase which relate to repeated component movements rather than to their specific order in a sequence in early phases of experience (Karni et al., 1995, 1998). The

absence of coherent RS effects across blocks for the U-FOS in the current study may, therefore, reflect the prior experience with the component movements that underwent stabilization overnight. Nevertheless, there were significant reductions in the M1 activity within the initial blocks of the pairs, that is, from the first to the second phase (Figures 4A and 5A), during the U-FOS performance. Repetition-related reductions in neural activity were also observed in perceptual systems (for a review, see Grill-Spector, Henson, & Martin, 2006) and were suggested to reflect tuning and task optimization processes (Schacter & Buckner, 1998; Wiggs & Martin, 1998; Desimone, 1996). From this point of view, the activity of cells that poorly represent the stimulus-specific features is reduced upon repetition, leaving cells carrying critical information for task performance (Desimone, 1996). We propose that the reduction of the M1 activity within the initial blocks reflects the tuning (i.e., adaptation) of the M1 representation for the novel sequence of movements. This within-block adaptation-like effect saturated by the second phase of the first block and did not recur across the brief rest interval, that is, BOLD signal levels, tended to stabilize during the second, repeated block. These modulations, during the performance of the U-FOS but not the T-FOS, presumably reflect the short-term accumulation of experience with the novel order (sequence, syntax) of movements as both sequences were composed of the same component opposition movements. It has been shown that the initial phases of motor task acquisition are characterized by various activity patterns of movement-related neurons selected and engaged from a more extensive pool in motor cortex; these activity patterns stabilize and a more restricted population is consistently engaged after extensive training (Peters et al., 2014). The transient stabilization of neural activity upon repeated performance blocks, in the current study, may result from the selection of a particular subset of excitatory neurons that were "tried out" during the corresponding initial blocks.

Our results suggest that the initial acquisition (encoding) of procedural knowledge about a novel order (sequencing) of component movements is characterized not only by short-term stabilizations of activity but also by an increase in functional connectivity between voxels within M1. An increase in functional connectivity within the primary motor cortex was previously observed during learning new muscle synergies (McNamara et al., 2007) and, recently, following noninvasive cortical stimulation using transcranial direct current stimulation (Sehm, Kipping, Schäfer, Villringer, & Ragert, 2013; Polanía, Paulus, & Nitsche, 2012). The increase of coherence and the transient signal stabilization within the M1 may be the neural signature of working memory processes (Fuster, 2001) whereby relevant information about the sequence of movements is maintained "in mind" for brief periods of time (Langner et al., 2013). There is evidence that M1 is capable of storing procedural information in STM (Classen, Liepert, Wise, Hallett, & Cohen, 1998). The capacity of the primary motor cortex to undergo short-term (transient) plastic modifications by practiced movements has been proposed to constitute the first step in skill acquisition and may be crucial for the long-term formation of a new motor skill representation (Classen et al., 1998; Karni et al., 1995). Differential repetition-driven short-term plasticity in M1 may be related to short-term modulations of GABA concentration and excitatory–inhibitory balance changes in relation to practice (Stagg, Bachtiar, & Johansen-Berg, 2011; Floyer-Lea, Wylezinska, Kincses, & Matthews, 2006; Bütefisch, Khurana, Kopylev, & Cohen, 2004). It has been suggested that rapid, regionally specific short-term decreases in GABA concentration in M1 may be associated primarily with encoding of the task during the period of task performance, rather than its longer-term consolidation (Floyer-Lea et al., 2006).

The fMRI-BOLD signal correlations between the right M1 hand area and the posterior ventral striatum, corresponding to the sensorimotor territories of the BG (Lehéricy et al., 2004, 2005), showed a differential pattern for the two sequences. For the U-FOS, there were relative increases in the right-M1–striatum connectivity after the brief rest interval. Repetition of the T-FOS resulted in relative decreases in the right-M1–striatum connectivity across blocks. The differential modulations of the M1–striatum connectivity upon repeated performance of the U-FOS compared with the T-FOS are in line with the notion that cortical and striatal circuits exhibit remarkable but dissociable plasticity as a function of the level of prior experience with a given task (Costa, Cohen, & Nicolelis, 2004). It has been proposed that high-level associative circuits with frontoparietal regions and associative regions of the striatum and the cerebellum are recruited during the early phase of motor learning, whereas sensorimotor regions may take over during later learning phases (Doyon et al., 2009; Doyon & Benali, 2005; Hikosaka, Nakamura, Sakai, & Nakahara, 2002). However, a dynamic shift of activation from the associative to the sensorimotor territories of the striatopallidal complex may occur early during training (Lehéricy et al., 2005). Lesions of the sensorimotor striatum in mice lead to significant and selective deficit in the acquisition of serial order in lever pressing (Yin, 2010).

Additional, albeit less robust, sequence-specific changes were found in functional connectivity of the right M1 hand area with the IFGa (BA 45 and 47). This region corresponds to Broca's area (Broca, 1861) and was implicated in various motor functions such as planning, recognition and imitation of actions (for reviews, see Fadiga, Craighero, & D'Ausilio, 2009; Binkofski & Buccino, 2006). The relative increase in functional connectivity between the right M1 hand area and the left IFGa during the U-FOS performance may reflect a recruitment of syntactic processing routines within the dominant hemisphere (Roy et al., 2013; Fazio et al., 2009) in early stages of sequence practice. On the other hand, the relative reduction in the coupling of the right M1 with the IFGa and the PMv across performance

blocks during the performance of the T-FOS may reflect a reduction in allocation of cognitive resources presumably involved in task aspects such as explicit sequence control and attention (Barber, Caffo, Pekar, & Mostofsky, 2013; Hikosaka et al., 2002; Honda et al., 1998).

The most common application of functional connectivity is examining intrinsic correlations determined during task-free intervals (rest). It has been proposed that resting-state functional connectivity approaches can not only reveal the underlying anatomical connectivity but also contribute to our understanding of brain dynamics (Deco, Jirsa, & McIntosh, 2011; Raichle, 2010). Although functional connectivity during rest may be significantly altered by motor learning (Vahdat et al., 2011; Albert, Robertson, & Miall, 2009), it may also be modified by rote button presses (Tung et al., 2013). Significant changes in functional connectivity patterns were observed for resting-state data, across imaging sessions (Honey et al., 2009), between runs within the same imaging session (Shehzad et al., 2009) as well as within the same run on a timescale of seconds to minutes (Chang & Glover, 2011) with no specific learning experience afforded. Thus, the assessment of functional connectivity during performance intervals, rather than during rest, may more directly reflect task-specific mnemonic processes.

It is not known whether and how the length and nature of the rest interval inserted between the two performance blocks affect the modulation of neural activity and connectivity upon task repetition. The number and rate of task iterations (the block length) may also be important factors in the modulation of BOLD signal to task repetition; however, the effects of changing these time parameters remain to be determined. Adaptation studies in the visual system showed that the magnitude of repetition effects was decreased with longer ISIs (Henson, Shallice, & Dolan, 2000; Grill-Spector et al., 1999) and increased with longer exposures to the stimuli (Grill-Spector et al., 1999). Robust repetition effects were observed in M1 and can be reproduced (recovered) in successive runs when these are separated by breaks (1.5–2 min) dedicated to verbal interaction with participants (Gabitov et al., 2014; Karni et al., 1995, 1998). One cannot rule out, however, that the verbal interaction with the participants during the breaks between runs may have an effect on the recovery of the repetition effects.

In the current study, the performance of the untrained sequence was significantly slower, less accurate, and more variable than the performance of the trained sequence, composed of identical opposition movements (Figure 7). However, during the scanning session, the differences in the rate of sequence execution and accuracy were minimized, because participants performed the component movements of both sequences at a comfortable, externally paced rate. Thus, the differences in patterns of modulation in neural activity and connectivity were not directly related to task execution speed or the number and nature of the component movements, but more likely reflected the differences in prior experience with the two sequences.

The behavioral data acquired immediately after the fMRI session suggest that the imaging session constituted a learning experience; experience with the U-FOS inside the scanner contributed to its faster performance and led to saturation of within-test improvements compared with the control group (Figure 7). The less accurate performance of the U-FOS in the fMRI group compared with the controls may be a consequence of proactive interference from the previously learned T-FOS (Cothros et al., 2006) or task-switching costs (Kiesel et al., 2010). The additional experience afforded during the fMRI session with the T-FOS had no significant impact on its subsequent performance.

Conclusions

Altogether, the current results support the idea that temporal signal modulations can reflect nonrandom consistent differential patterns of brain activity evolving as a function of the statistics of accumulated experience. Brain function may be underappreciated when using mean-based brain measures (He, 2013; Garrett et al., 2010, 2011; Stein et al., 2005), but measures of signal variability per se may not reflect critical aspects of experience-driven changes in brain activity. We propose that a network including M1 and striatum underlies online motor working memory whereby motor representations of specific movement sequences are retained across short periods of time (Langner et al., 2013). This network may promote a transient integrated representation of a new movement sequence and readily retrieves a previously established movement sequence representation.

Acknowledgments

E. G. was partially supported by a fellowship from the E. J. Safra Brain Research Center for the Study of Learning Disabilities. The research leading to these results has received funding from the European Union Seventh Framework Program (FP7/2007-2013) under grant agreement no. 604102 (Human Brain Project). We thank Tammi Kushnir, Ph.D., director of research at the C. Sheba Medical Center, for her technical and administrative support.

Reprint requests should be sent to Ella Gabitov, University of Haifa, 199 Abba Hushi Blvd., Mount Carmel, Haifa 3498838, Israel, or via e-mail: gabitovella@gmail.com.

REFERENCES

Albert, N. B., Robertson, E. M., & Miall, R. C. (2009). The resting human brain and motor learning. *Current Biology, 19,* 1023–1027.

Andersson, J. L. R., Hutton, C., Ashburner, J., Turner, R., & Friston, K. J. (2001). Modeling geometric deformations in EPI time series. *Neuroimage, 13,* 903–919.

Barber, A. D., Caffo, B. S., Pekar, J. J., & Mostofsky, S. H. (2013). Effects of working memory demand on neural

mechanisms of motor response selection and control. *Journal of Cognitive Neuroscience, 25,* 1235–1248.
Ben-Shaul, Y., Drori, R., Asher, I., Stark, E., Nadasdy, Z., & Abeles, M. (2004). Neuronal activity in motor cortical areas reflects the sequential context of movement. *Journal of Neurophysiology, 91,* 1748–1762.
Bestmann, S., Swayne, O., Blankenburg, F., Ruff, C. C., Haggard, P., Weiskopf, N., et al. (2008). Dorsal premotor cortex exerts state-dependent causal influences on activity in contralateral primary motor and dorsal premotor cortex. *Cerebral Cortex, 18,* 1281–1291.
Binkofski, F., & Buccino, G. (2006). The role of ventral premotor cortex in action execution and action understanding. *Journal of Physiology Paris, 99,* 396–405.
Brett, M., Anton, J.-L., Valabregue, R., & Poline, J.-B. (2002). *Region of interest analysis using an SPM toolbox [abstract]*. Presented at the 8th International Conference on Functional Mapping of the Human Brain, June 2–6, 2002, Sendai, Japan. Available on CD-ROM in Neuroimage, Vol 16.
Broca, P. P. (1861). Remarques sur le siège de la faculté du langage articulé; suivies d'une observation d'aphémie, 1861. *Bulletin de la Société Anatomique (Paris), 2,* 330–357.
Bütefisch, C. M., Khurana, V., Kopylev, L., & Cohen, L. G. (2004). Enhancing encoding of a motor memory in the primary motor cortex by cortical stimulation. *Journal of Neurophysiology, 91,* 2110–2116.
Carpenter, A. F., Georgopoulos, A. P., & Pellizzer, G. (1999). Motor cortical encoding of serial order in a context-recall task. *Science, 283,* 1752–1757.
Chang, C., & Glover, G. H. (2011). Time-frequency dynamics of resting-state brain connectivity measured with fMRI. *Neuroimage, 50,* 81–98.
Chouinard, P. A., & Goodale, M. A. (2009). fMRI adaptation during performance of learned arbitrary visuomotor conditional associations. *Neuroimage, 48,* 696–706.
Churchland, M. M., Yu, B. M., Cunningham, J. P., Sugrue, L. P., Cohen, M. R., Corrado, G. S., et al. (2010). Stimulus onset quenches neural variability: A widespread cortical phenomenon. *Nature Neuroscience, 13,* 369–378.
Churchland, M. M., Yu, B. M., Ryu, S. I., Santhanam, G., & Shenoy, K. V. (2006). Neural variability in premotor cortex provides a signature of motor preparation. *Journal of Neuroscience, 26,* 3697–3712.
Classen, J., Liepert, J., Wise, S. P., Hallett, M., & Cohen, L. G. (1998). Rapid plasticity of human cortical movement representation induced by practice. *Journal of Neurophysiology, 79,* 1117–1123.
Costa, R. M., Cohen, D., & Nicolelis, M. A. L. (2004). Differential corticostriatal plasticity during fast and slow motor skill learning in mice. *Current Biology, 14,* 1124–1134.
Cothros, N., Köhler, S., Dickie, E. W., Mirsattari, S. M., & Gribble, P. L. (2006). Proactive interference as a result of persisting neural representations of previously learned motor skills in primary motor cortex. *Journal of Cognitive Neuroscience, 18,* 2167–2176.
Davare, M., Lemon, R. N., & Olivier, E. (2008). Selective modulation of interactions between ventral premotor cortex and primary motor cortex during precision grasping in humans. *Journal of Physiology, 586,* 2735–2742.
Davare, M., Montague, K., Olivier, E., Rothwell, J. C., & Lemon, R. N. (2009). Ventral premotor to primary motor cortical interactions during object-driven grasp in humans. *Cortex, 45,* 1050–1057.
Deco, G., Jirsa, V. K., & McIntosh, A. R. (2011). Emerging concepts for the dynamical organization of resting-state activity in the brain. *Nature Reviews Neuroscience, 12,* 43–56.
Desimone, R. (1996). Neural mechanisms for visual memory and their role in attention. *Proceedings of the National Academy of Sciences, U.S.A., 93,* 13494–13499.
Dinstein, I., Hasson, U., Rubin, N., & Heeger, D. J. (2007). Brain areas selective for both observed and executed movements. *Journal of Neurophysiology, 98,* 1415–1427.
Doyon, J., Bellec, P., Amsel, R., Penhune, V. B., Monchi, O., Carrier, J., et al. (2009). Contributions of the basal ganglia and functionally related brain structures to motor learning. *Behavioural Brain Research, 199,* 61–75.
Doyon, J., & Benali, H. (2005). Reorganization and plasticity in the adult brain during learning of motor skills. *Current Opinion in Neurobiology, 15,* 161–167.
Fadiga, L., Craighero, L., & D'Ausilio, A. (2009). Broca's area in language, action, and music. *Annals of the New York Academy of Sciences, 1169,* 448–458.
Fazio, P., Cantagallo, A., Craighero, L., D'Ausilio, A., Roy, A. C., Pozzo, T., et al. (2009). Encoding of human action in Broca's area. *Brain, 132,* 1980–1988.
Fedorenko, E., Hsieh, P.-J., Nieto-Castañón, A., Whitfield-Gabrieli, S., & Kanwisher, N. (2010). New method for fMRI investigations of language: Defining ROIs functionally in individual subjects. *Journal of Neurophysiology, 104,* 1177–1194.
Floyer-Lea, A., & Matthews, P. M. (2005). Distinguishable brain activation networks for short- and long-term motor skill learning. *Journal of Neurophysiology, 94,* 512–518.
Floyer-Lea, A., Wylezinska, M., Kincses, T., & Matthews, P. M. (2006). Rapid modulation of GABA concentration in human sensorimotor cortex during motor learning. *Journal of Neurophysiology, 95,* 1639–1644.
Friston, K. J., Holmes, A. P., Worsley, K. J., Poline, J.-B., Frith, C. D., & Frackowiak, R. S. J. (1995). Statistical parametric maps in functional imaging: A general linear approach. *Human Brain Mapping, 2,* 189–210.
Fuster, J. M. (2001). The prefrontal cortex—An update: Time is of the essence. *Neuron, 30,* 319–333.
Gabitov, E., Manor, D., & Karni, A. (2014). Done that: Short-term repetition related modulations of motor cortex activity as a stable signature for overnight motor memory consolidation. *Journal of Cognitive Neuroscience, 26,* 2716–2734.
Garrett, D. D., Kovacevic, N., McIntosh, A. R., & Grady, C. L. (2010). Blood oxygen level-dependent signal variability is more than just noise. *Journal of Neuroscience, 30,* 4914–4921.
Garrett, D. D., Kovacevic, N., McIntosh, A. R., & Grady, C. L. (2011). The importance of being variable. *Journal of Neuroscience, 31,* 4496–4503.
Georgopoulos, A. P., Kalaska, J. F., Caminiti, R., & Massey, J. T. (1982). On the relations between the direction of two-dimensional arm movements and cell discharge in primate motor cortex. *Journal of Neuroscience, 2,* 1527–1537.
Grafton, S. T., & Hamilton, A. F. (2007). Evidence for a distributed hierarchy of action representation in the brain. *Human Movement Science, 26,* 590–616.
Grill-Spector, K., Henson, R. N., & Martin, A. (2006). Repetition and the brain: Neural models of stimulus-specific effects. *Trends in Cognitive Sciences, 10,* 14–23.
Grill-Spector, K., Kushnir, T., Edelman, S., Avidan, G., Itzchak, Y., & Malach, R. (1999). Differential processing of objects under various viewing conditions in the human lateral occipital complex. *Neuron, 24,* 187–203.
Halsband, U., & Lange, R. K. (2006). Motor learning in man: A review of functional and clinical studies. *Journal of Physiology-Paris, 99,* 414–424.
Hamilton, A. F., & Grafton, S. T. (2009). Repetition suppression for performed hand gestures revealed by fMRI. *Human Brain Mapping, 30,* 2898–2906.

Hardwick, R. M., Rottschy, C., Miall, R. C., & Eickhoff, S. B. (2013). A quantitative meta-analysis and review of motor learning in the human brain. *Neuroimage, 67,* 283–297.
Hatsopoulos, N. G., Paninski, L., & Donoghue, J. P. (2003). Sequential movement representations based on correlated neuronal activity. *Experimental Brain Research, 149,* 478–486.
He, B. J. (2013). Spontaneous and task-evoked brain activity negatively interact. *Journal of Neuroscience, 33,* 4672–4682.
Henson, R. N., Shallice, T., & Dolan, R. (2000). Neuroimaging evidence for dissociable forms of repetition priming. *Science, 287,* 1269–1272.
Hikosaka, O., Nakamura, K., Sakai, K., & Nakahara, H. (2002). Central mechanisms of motor skill learning. *Current Opinion in Neurobiology, 12,* 217–222.
Honda, M., Deiber, M.-P., Ibáñez, V., Pascual-Leone, A., Zhuang, P., & Hallett, M. (1998). Dynamic cortical involvement in implicit and explicit motor sequence learning. A PET study. *Brain, 121,* 2159–2173.
Honey, C. J., Sporns, O., Cammoun, L., Gigandet, X., Thiran, J.-P., Meuli, R. A., et al. (2009). Predicting human resting-state functional connectivity from structural connectivity. *Proceedings of the National Academy of Sciences, U.S.A., 106,* 2035–2040.
Hutton, C., Andersson, J., Deichmann, R., & Weiskopf, N. (2013). Phase informed model for motion and susceptibility. *Human Brain Mapping, 34,* 3086–3100.
Johnstone, T., Ores Walsh, K. S., Greischar, L. L., Alexander, A. L., Fox, A. S., Davidson, R. J., et al. (2006). Motion correction and the use of motion covariates in multiple-subject fMRI analysis. *Human Brain Mapping, 27,* 779–788.
Kantak, S. S., Mummidisetty, C. K., & Stinear, J. W. (2012). Primary motor and premotor cortex in implicit sequence learning-evidence for competition between implicit and explicit human motor memory systems. *European Journal of Neuroscience, 36,* 2710–2715.
Karni, A., Meyer, G., Jezzard, P., Adams, M. M., Turner, R., & Ungerleider, L. G. (1995). Functional MRI evidence for adult motor cortex plasticity during motor skill learning. *Nature, 377,* 155–158.
Karni, A., Meyer, G., Rey-Hipolito, C., Jezzard, P., Adams, M. M., Turner, R., et al. (1998). The acquisition of skilled motor performance: Fast and slow experience-driven changes in primary motor cortex. *Proceedings of the National Academy of Sciences, U.S.A., 95,* 861–868.
Kiesel, A., Steinhauser, M., Wendt, M., Falkenstein, M., Jost, K., Philipp, A. M., et al. (2010). Control and interference in task switching—A review. *Psychological Bull, 136,* 849–874.
Kim, Y.-H., Park, J.-W., Ko, M.-H., Jang, S. H., & Lee, P. K. W. (2004). Facilitative effect of high frequency subthreshold repetitive transcranial magnetic stimulation on complex sequential motor learning in humans. *Neuroscience Letters, 367,* 181–185.
Kleim, J. A., Hogg, T. M., VandenBerg, P. M., Cooper, N. R., Bruneau, R., & Remple, M. (2004). Cortical synaptogenesis and motor map reorganization occur during late, but not early, phase of motor skill learning. *Journal of Neuroscience, 24,* 628–633.
Korman, M., Doyon, J., Doljansky, J., Carrier, J., Dagan, Y., & Karni, A. (2007). Daytime sleep condenses the time course of motor memory consolidation. *Nature Neuroscience, 10,* 1206–1213.
Korman, M., Raz, N., Flash, T., & Karni, A. (2003). Multiple shifts in the representation of a motor sequence during the acquisition of skilled performance. *Proceedings of the National Academy of Sciences, U.S.A., 100,* 12492–12497.
Langner, R., Sternkopf, M. A., Kellermann, T. S., Grefkes, C., Kurth, F., Schneider, F., et al. (2013). Translating working memory into action: Behavioral and neural evidence for using motor representations in encoding visuo-spatial sequences. *Human Brain Mapping, 35,* 3465–3484.
Lehéricy, S., Benali, H., Van de Moortele, P.-F., Pélégrini-Issac, M., Waechter, T., Ugurbil, K., et al. (2005). Distinct basal ganglia territories are engaged in early and advanced motor sequence learning. *Proceedings of the National Academy of Sciences, U.S.A., 102,* 12566–12571.
Lehéricy, S., Ducros, M., Krainik, A., Francois, C., Van de Moortele, P.-F., Ugurbil, K., et al. (2004). 3-D diffusion tensor axonal tracking shows distinct SMA and pre-SMA projections to the human striatum. *Cerebral Cortex, 14,* 1302–1309.
Matsuzaka, Y., Picard, N., & Strick, P. L. (2007). Skill representation in the primary motor cortex after long-term practice. *Journal of Neurophysiology, 97,* 1819–1832.
Mayka, M. A., Corcos, D. M., Leurgans, S. E., & Vaillancourt, D. E. (2006). Three-dimensional locations and boundaries of motor and premotor cortices as defined by functional brain imaging: A meta-analysis. *Neuroimage, 31,* 1453–1474.
Mazaika, P. K., Hoeft, F., Glover, G. H., & Reiss, A. L. (2009). Methods and software for fMRI analysis of clinical subjects. *Annual Meeting of the Organization for Human Brain Mapping*. doi:10.1016/S1053-8119(09)70238-1.
McNamara, A., Tegenthoff, M., Dinse, H., Büchel, C., Binkofski, F., & Ragert, P. (2007). Increased functional connectivity is crucial for learning novel muscle synergies. *Neuroimage, 35,* 1211–1218.
Mohr, P. N. C., & Nagel, I. E. (2010). Variability in brain activity as an individual difference measure in neuroscience? *Journal of Neuroscience, 30,* 7755–7757.
Nieto-Castañón, A., & Fedorenko, E. (2012). Subject-specific functional localizers increase sensitivity and functional resolution of multi-subject analyses. *Neuroimage, 63,* 1646–1669.
Nitsche, M. A., Schauenburg, A., Lang, N., Liebetanz, D., Exner, C., Paulus, W., et al. (2003). Facilitation of implicit motor learning by weak transcranial direct current stimulation of the primary motor cortex in the human. *Journal of Cognitive Neuroscience, 15,* 619–626.
Nudo, R. J., Jenkins, W. M., Prejean, T., & Grenda, R. (1992). Neurophysiological correlates of hand preference in primary motor cortex of adult squirrel monkeys. *Journal of Neuroscience, 12,* 2918–2947.
Nudo, R. J., Milliken, G. W., Jenkins, W. M., & Merzenich, M. M. (1996). Use-dependent alterations of movement representations in primary motor cortex of adult squirrel monkeys. *Journal of Neuroscience, 16,* 785–807.
Oldfield, R. C. (1971). The assessment and analysis of handedness: The Edinburgh inventory. *Neuropsychologia, 9,* 97–113.
Orban, P., Peigneux, P., Lungu, O., Debas, K., Barakat, M., Bellec, P., et al. (2011). Functional neuroanatomy associated with the expression of distinct movement kinematics in motor sequence learning. *Neuroscience, 179,* 94–103.
Penhune, V. B., & Doyon, J. (2002). Dynamic cortical and subcortical networks in learning and delayed recall of timed motor sequences. *Journal of Neuroscience, 22,* 1397–1406.
Penhune, V. B., & Doyon, J. (2005). Cerebellum and M1 interaction during early learning of timed motor sequences. *Neuroimage, 26,* 801–812.
Peters, A. J., Chen, S. X., & Komiyama, T. (2014). Emergence of reproducible spatiotemporal activity during motor learning. *Nature, 510,* 263–267.
Polanía, R., Paulus, W., & Nitsche, M. A. (2012). Reorganizing the intrinsic functional architecture of the human primary

motor cortex during rest with non-invasive cortical stimulation. *PloS One, 7,* e30971.
Poldrack, R. A. (2000). Imaging brain plasticity: Conceptual and methodological issues—A theoretical review. *Neuroimage, 12,* 1–13.
Raichle, M. E. (2010). Two views of brain function. *Trends in Cognitive Sciences, 14,* 180–190.
Rao, S. M., Bandettini, P. A., Binder, J. R., Bobholz, J. A., Hammeke, T. A., Stein, E. A., et al. (1996). Relationship between finger movement rate and functional magnetic resonance signal change in human primary motor cortex. *Journal of Cerebral Blood Flow & Metabolism, 16,* 1250–1254.
Roy, A. C., Curie, A., Nazir, T., Paulignan, Y., des Portes, V., Fourneret, P., et al. (2013). Syntax at hand: Common syntactic structures for actions and language. *PloS One, 8,* e72677.
Saucedo Marquez, C. M., Zhang, X., Swinnen, S. P., Meesen, R., & Wenderoth, N. (2013). Task-specific effect of transcranial direct current stimulation on motor learning. *Frontiers in Human Neuroscience, 7.* doi:10.3389/fnhum.2013.00333.
Schacter, D. L., & Buckner, R. L. (1998). Priming and the brain review. *Neuron, 20,* 185–195.
Schlaug, G., Knorr, U., & Seitz, R. J. (1994). Inter-subject variability of cerebral activations in acquiring a motor skill: A study with positron emission tomography. *Experimental Brain Research, 98,* 523–534.
Sehm, B., Kipping, J., Schäfer, A., Villringer, A., & Ragert, P. (2013). A comparison between uni- and bilateral tDCS effects on functional connectivity of the human motor cortex. *Frontiers in Human Neuroscience, 7.* doi:10.3389/fnhum.2013.00183.
Shehzad, Z., Kelly, A. M. C., Reiss, P. T., Gee, D. G., Gotimer, K., Uddin, L. Q., et al. (2009). The resting brain: Unconstrained yet reliable. *Cerebral Cortex, 19,* 2209–2229.
Stagg, C. J., Bachtiar, V., & Johansen-Berg, H. (2011). The role of GABA in human motor learning. *Current Biology, 21,* 480–484.
Stagg, C. J., Jayaram, G., Pastor, D., Kincses, Z. T., Matthews, P. M., & Johansen-Berg, H. (2011). Polarity and timing-dependent effects of transcranial direct current stimulation in explicit motor learning. *Neuropsychologia, 49,* 800–804.
Steele, C. J., & Penhune, V. B. (2010). Specific increases within global decreases: A functional magnetic resonance imaging investigation of five days of motor sequence learning. *Journal of Neuroscience, 30,* 8332–8341.
Stein, R. B., Gossen, E. R., & Jones, K. E. (2005). Neuronal variability: Noise or part of the signal? *Nature Reviews Neuroscience, 6,* 389–397.
Tanji, J. (2001). Sequential organization of multiple movements: Involvement of cortical motor areas. *Annual Review of Neuroscience, 24,* 631–651.
Toni, I., Krams, M., Turner, R., & Passingham, R. E. (1998). The time course of changes during motor sequence learning: A whole-brain fMRI study. *Neuroimage, 8,* 50–61.
Tung, K.-C., Uh, J., Mao, D., Xu, F., Xiao, G., & Lu, H. (2013). Alterations in resting functional connectivity because of recent motor task. *Neuroimage, 78,* 316–324.
Tzourio-Mazoyer, N., Landeau, B., Papathanassiou, D., Crivello, F., Etard, O., Delcroix, N., et al. (2002). Automated anatomical labeling of activations in SPM using a macroscopic anatomical parcellation of the MNI MRI single-subject brain. *Neuroimage, 15,* 273–289.
Vahdat, S., Darainy, M., Milner, T. E., & Ostry, D. J. (2011). Functionally specific changes in resting-state sensorimotor networks after motor learning. *Journal of Neuroscience, 31,* 16907–16915.
Vines, B. W., Nair, D. G., & Schlaug, G. (2006). Contralateral and ipsilateral motor effects after transcranial direct current stimulation. *NeuroReport, 17,* 671–674.
Von Neumann, J., Kent, R. H., Bellinson, H. R., & Hart, B. I. (1941). The mean square successive difference. *Annals of Mathematical Statistics, 12,* 153–162.
White, B., Abbott, L. F., & Fiser, J. (2012). Suppression of cortical neural variability is stimulus- and state-dependent. *Journal of Neurophysiology, 108,* 2383–2392.
Whitfield-Gabrieli, S., & Nieto-Castanon, A. (2012). Conn: A functional connectivity toolbox for correlated and anticorrelated brain networks. *Brain Connectivity, 2,* 125–141.
Wiggs, C. L., & Martin, A. (1998). Properties and mechanisms of perceptual priming. *Current Opinion in Neurobiology, 8,* 227–233.
Woods, R. P. (1996). Modeling for intergroup comparisons of imaging data. *Neuroimage, 4,* S84–S94.
Xu, T., Yu, X., Perlik, A. J., Tobin, W. F., Zweig, J. A., Tennant, K. A., et al. (2009). Rapid formation and selective stabilization of synapses for enduring motor memories. *Nature, 462,* 915–919.
Yang, G., Lai, C. S. W., Cichon, J., Ma, L., Li, W., & Gan, W.-B. (2014). Sleep promotes branch-specific formation of dendritic spines after learning. *Science, 344,* 1173–1178.
Yang, G., Pan, F., & Gan, W.-B. (2009). Stably maintained dendritic spines are associated with lifelong memories. *Nature, 462,* 920–924.
Yin, H. H. (2010). The sensorimotor striatum is necessary for serial order learning. *Journal of Neuroscience, 30,* 14719–14723.
Yousry, T. A., Schmid, U. D., Alkadhi, H., Schmidt, D., Peraud, A., Buettner, A., et al. (1997). Localization of the motor hand area to a knob on the precentral gyrus. A new landmark. *Brain, 120,* 141–157.
Zelenin, P. V., Deliagina, T. G., Orlovsky, G. N., Karayannidou, A., Stout, E. E., Sirota, M. G., et al. (2011). Activity of motor cortex neurons during backward locomotion. *Journal of Neurophysiology, 105,* 2698–2714.